Journal of Thermal Analysis and Calorimetry, Vol. 91 (2008) 3, 687–695

VITRIFICATION DURING THE ISOTHERMAL CURE OF THERMOSETS Part I. An investigation using TOPEM, a new temperature modulated technique

I. Fraga, S. Montserrat and J. M. Hutchinson[*]

Departament de Màquines i Motors Tèrmics, ETSEIAT, Universitat Politècnica de Catalunya, Colom 11, 08222 Terrassa, Spain

The process of vitrification that occurs during the isothermal cure of a cross-linking system at temperatures below $T_{g\infty}$, the glass transition temperature of the fully cured resin, has been studied by TOPEM, a new temperature modulated DSC (TMDSC) technique based upon the use of stochastic temperature pulses. A comparison is made between TOPEM and another TMDSC technique, and some advantages of TOPEM are considered. The TOPEM technique is used to show that the mobility factor is not always a reliable approach to predicting the cure rate during vitrification, in view of its frequency dependence. Also, the dependence of the apparent vitrification time on frequency is examined. There appears to be a non-linear relationship between the apparent vitrification time and log(frequency), which is further discussed in the second part of this series.

Keywords: *cure of thermosets, TMDSC, TOPEM, vitrification*

Introduction

In the isothermal curing of thermosets, the reaction initially proceeds at a rate which depends in general on the degree of cure and on the temperature dependent rate constant of the chemical reaction involved. As the degree of cure α increases from zero, the glass transition temperature of the curing thermoset also increases from its original value, T_{g0}, namely that of the unreacted mixture of the monomer and cross-linking agent. If the cure temperature is sufficiently high, the cross-linking reaction will proceed to its limit, α=1, and the final glass transition will be that of the fully cured thermoset, $T_{g\infty}$. The relationship between the glass transition and the degree of cure at any time during the cross-linking reaction can be described by, for example, the DiBenedetto equation [1]. On the other hand, if the cure temperature is less than $T_{g\infty}$, then there occurs a change in the overall rate of reaction from the initial chemically controlled rate to one that is controlled by the rate of diffusion of the reacting species. The change occurs roughly when the glass transition temperature of the curing thermoset reaches the isothermal cure temperature, because any further reaction implies the transition from a liquid state with high molecular mobility to a glassy state with much lower molecular mobility. This dramatic slowing down of the rate of reaction is known as vitrification, and it is conventional to assign the vitrification time as that for which the glass transition of the curing thermoset is equal to the cure temperature. A knowledge of the vitrification time and its dependence on the cure temperature is important, for example, in the construction of time–temperature–transformation (*TTT*) diagrams [2].

The experimental determination of the vitrification time by conventional differential scanning calorimetry (DSC) for any given cure temperature is a very time-consuming process. It requires a series of separate isothermal cure experiments, at the same cure temperature but for increasing cure times, in which the system is only partially cured. Each isothermal experiment is followed immediately by a second DSC scan at constant heating rate, from which the glass transition temperature of the partially cured system is evaluated. Plotting this temperature as a function of the cure time (on a logarithmic scale) allows the determination of the vitrification time. A good illustration of this procedure has been given by Montserrat [3]; each point in Fig. 4 of this reference requires both an isothermal cure and a second scan, from which the time-consuming nature of obtaining these data can be inferred.

The advent of temperature modulated DSC (TMDSC) techniques such as Modulated DSC (MDSC, TA Instruments) or Alternating DSC (ADSC, Mettler-Toledo), considerably simplified such experiments. In addition to the total heat flow given by conventional DSC, TMDSC also allows the determination, continuously throughout the reaction, of the so-called complex heat capacity, C_p^*, from the heat flow response to the small amplitude temperature modulations superimposed on the isotherm. When the curing system vitrifies, C_p^* changes gradually from a value corresponding to the liquid state to a lower value

* Author for correspondence: hutchinson@mmt.upc.edu

1388–6150/$20.00

Akadémiai Kiadó, Budapest, Hungary
Springer, Dordrecht, The Netherlands

corresponding to the glassy state. It therefore appears possible, from a single TMDSC quasi-isothermal experiment, to follow both the overall heat of curing as in conventional DSC and the vitrification process. In this case, the vitrification time, t_v, is conventionally defined as the time at which the value of C_p^* is mid-way between those of the liquid and glassy states. This t_v will not in general be exactly the same as the vitrification time defined by when the glass transition temperature is equal to the cure temperature, but the correspondence is often sufficiently close for the difference to be immaterial in the present context, even though there are notable exceptions which will be discussed later. Good illustrations of the application of TMDSC to the study of the vitrification process may be found in the publications of Cassettari *et al*. [4], Van Mele and Van Hemelrijck [5, 6] and Montserrat *et al*. [7, 8].

The reason why t_v from TMDSC is not in general exactly the same as that from conventional DSC is considered in detail below, but is essentially related to the frequency and rate dependences of the glass transition, in other words of the α-relaxation [9, 10]. Hence the study of the frequency dependence of the vitrification time is of interest, and t_v determined from TMDSC techniques will here be referred to as the 'dynamic vitrification time' in order to distinguish it from that defined by the change from a chemically controlled reaction rate to one controlled by diffusion.

For the determination of the dynamic vitrification time, the techniques of MDSC and ADSC can exhibit some drawbacks. In particular, ADSC experiments are conducted at a single fixed frequency. The study of the frequency dependence of the dynamic vitrification time therefore requires a series of separate ADSC experiments, together with their corresponding blank runs, at each of the frequencies to be investigated. Not only is this once again time-consuming but, in situations in which a significant, even if small, amount of cure takes place during the storage time required for the completion of the series of frequencies, it is not suitable to make a batch of the mixture of resin and cross-linking agent from which samples for curing can be taken. An example of this situation is found in the cure of epoxy-based polymer layered silicate nanocomposites, for which the organically modified clay catalyses the curing reaction [11]. Instead, it requires a fresh mixture of the resin and cross-linking agent to be made for each frequency, which introduces the possibility of small variations in the ratio of resin to cross-linking agent in each mixture, which would contribute to the experimental error. To avoid this, as well as to reduce the experimental time involved, a multi-frequency technique would be advantageous. This is provided by TOPEM, a new modulated DSC technique from Mettler-Toledo [12]. The purpose of the present work is to compare the study of the vitrification process by TOPEM and ADSC for the isothermal cure of an epoxy-diamine system.

Experimental

The epoxy resin used here was a diglycidyl ether of bisphenol-A (DGEBA), Epon 828 (Shell Chemicals, Resolution Performance Products), with a density of 1.16 g cm^{-3} and an epoxide equivalent (ee) mass in the range 185–192 g ee^{-1}. The cross-linking agent was a polyoxypropylene diamine, Jeffamine D-230 (Huntsman Corporation). Stoichiometric mixtures of resin and diamine were prepared and samples of suitable mass were weighed into aluminium crucibles. For TOPEM, the recommended sample mass of approximately 20 mg was used, while for ADSC the sample mass was dependent on the modulation period, increasing from about 7 mg for the shortest period (30 s) to about 26 mg for the longest (900 s).

The same calorimeter, Mettler-Toledo 823^e with an intracooler, was used for both ADSC and TOPEM experiments, the difference being simply in the software for the temperature programme and subsequent data analysis. Also for both techniques, the same isothermal cure temperatures of 50 and 70°C were used, the furnace in each case being preheated to the required temperature before the sample in the aluminium crucible was inserted by robot. The cure times were 14 or 15 h for 50°C and 10 to 12 h for 70°C, the longer cure times being used for the lower frequencies, for which vitrification occurs later. For ADSC mode, a temperature amplitude of 0.5 K was used, with modulation periods ranging from 30 to 900 s, and a blank run being made in addition to the sample run for each period. For TOPEM, the magnitude of the temperature pulse was 0.5 K, equivalent to an amplitude of ±0.25 K around the constant temperature baseline, and the random pulse durations, called the 'switching time range', were set to be in various ranges in order to investigate this experimental parameter: 15–30 s for cure at 50°C, and 15–30, 15–300, 15–600 and 15–900 s for cure at 70°C. The difference between the temperature amplitudes for ADSC and TOPEM is immaterial, as they are considered to be sufficiently small for the response to be linear [13].

Results

ADSC experiments

A typical result for an ADSC experiment is shown in Fig. 1 for a modulation period of 60 s and a cure temperature of 50°C. The dynamic vitrification time,

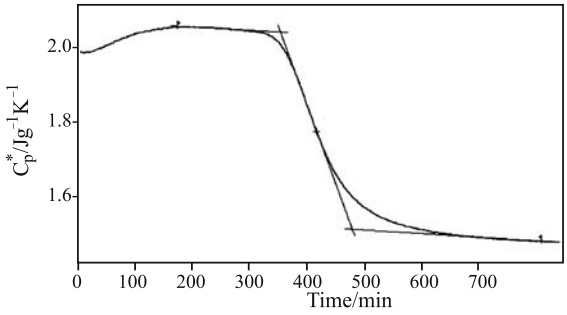

Fig. 1 Complex heat capacity, C_p^*, as a function of time for ADSC experiment with a modulation period of 60 s, a temperature amplitude of 0.5 K and a cure temperature of 50°C, showing the construction used to determine the dynamic vitrification time, t_v

Table 1 Dynamic vitrification times obtained from the mid-point of the C_p^* curves as a function of frequency (or period, in seconds, shown in parentheses) for quasi-isothermal ADSC experiments at 50 and 70°C with an amplitude of 0.5 K

Frequency/mHz	50°C	70°C
	t_v/min	t_v/min
33.3 (30)	406.7	223.1
16.7 (60)	418.8	237.3
8.3 (120)	425.1	255.3
3.3 (300)	447.5	279.9
1.7 (600)	–	319.7
1.1 (900)	–	322.6

t_v, is found as the mid-point of this curve, as illustrated. Similar results for other modulation periods allow the relationship between t_v and period (or frequency f=1/period) to be determined. This series of experiments was repeated for a cure temperature of 70°C, and the results for both cure temperatures are summarised in Table 1.

From the original modulated heat flow curves of the ADSC experiment it is also possible to determine the total heat flow due to the quasi-isothermal curing process, equivalent to the heat flow that would be measured in a conventional DSC experiment. This is shown in Fig. 2 for the cure temperature of 50°C. In fact, although it cannot be seen on the scale of this figure, the data start from 30 s rather than zero time, which results from the analysis procedure involving a window of width equal to one modulation period, the heat flow corresponding to this evaluation being associated with the time at the mid-point of this window. However, in this case, for which the period is 60 s, the heat of cure associated with this initial region is sufficiently small as to have a negligible effect. For much longer periods this is not necessarily the case, and hence the heat flow calculation is made only for the ADSC experiment with a period of 60 s.

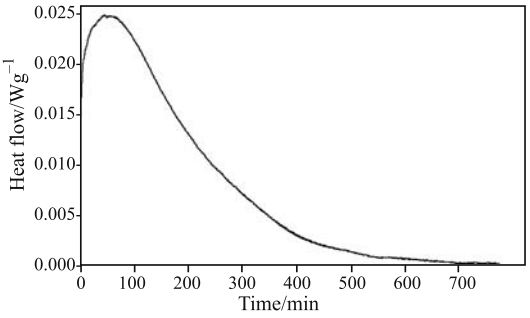

Fig. 2 Total heat flow from ADSC quasi-isothermal experiment at 50°C with modulation period of 60 s and temperature amplitude of 0.5 K

After each quasi-isothermal cure, the sample was heated in a conventional DSC scan at 10 K min^{-1} from 10 to 270°C to determine the residual heat of cure, with a further scan being made to determine the glass transition temperature, $T_{g\infty}$, of the fully cured sample.

TOPEM experiments

The TOPEM experiment measures the heat flow response to the stochastic temperature programme. The heat flow for quasi-isothermal cure at 70°C is illustrated in Fig. 3, with an enlarged view of the response to just a few temperature pulses shown in the inset. Here, the stochastic nature of the pulses can be seen in the random pulse durations (illustrated in the inset to Fig. 3) within the limits set by the switching time range (15 to 30 s in the present case). Similar to ADSC, following the quasi-isothermal cure, second and third conventional DSC scans were performed to determine the residual heat of cure and the $T_{g\infty}$, respectively.

The TOPEM evaluation procedure uses a parameter estimation method to determine the so-called quasi-static heat capacity, C_{p0}, from the relationship

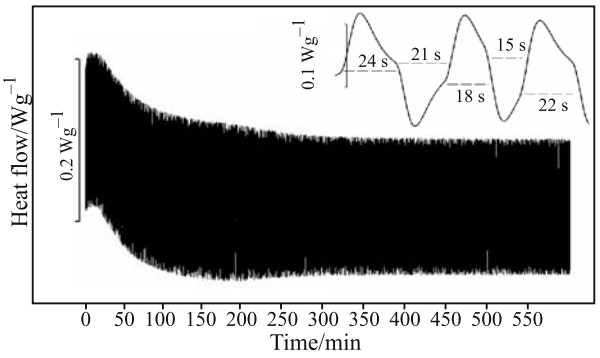

Fig. 3 Heat flow response of TOPEM to stochastic temperature pulses with switching time range of 15 to 30 s during quasi-isothermal cure at 70°C. The inset shows a magnified view of five pulses, of duration 24, 21, 18, 15 and 22 s

between the temperature programme and the heat flow response [12]. For this, a calculation window is used, which is then shifted in time along the heat flow response for successive evaluations of C_{p0}, with, finally, a smoothing of the C_{p0} data. This is analogous to the procedure for ADSC where the calculation window width is one modulation of the heating rate. In TOPEM, the three important evaluation parameters, namely the width of the calculation window, the shift of this window and the smoothing time range, are user-defined. The default values are, respectively, 120, 10 and 90 s.

The full line in Fig. 4 shows the curve for C_{p0} as a function of time obtained from the heat flow data of Fig. 3, using a calculation window width of 1200 s. Just as for ADSC, vitrification is identified by a sigmoidal change in C_{p0}. The next step in TOPEM is to isolate the required event, in this case the vitrification process, as shown by the outermost and upward-pointing flags in Fig. 4 (the positions of the innermost and downward-pointing flags are used to adjust the slopes of the asymptotes), and then select the frequencies required, in the present case 3.3, 8.3, 16.7 and 33.3 mHz, chosen so as to correspond to the modulation periods used with ADSC. In addition, for TOPEM at 70°C higher frequencies of 50, 66.7, 100 and 120 mHz were also selected. The software then allows TOPEM to determine the separate frequency-dependent C_p(f) curves, analogous to C_p^* in ADSC. The results are shown, together with C_{p0}, in Fig. 4. From this, and an equivalent experiment at 50°C, the values of the dynamic vitrification time at each frequency and for each isothermal cure temperature are determined, and the results are summarised in Table 2.

The total heat flow in a TOPEM experiment can be calculated either directly from the original heat flow data of Fig. 3 or from the sum of the reversing and non-reversing heat flow components, which may be determined independently [12] and hence serves as an internal check on the calculations. The result is very similar to that obtained for ADSC shown in Fig. 2, the initial part of the heat flow curve for TOPEM being truncated up to a time equal to half the width of the calculation window. Wide calculation windows, therefore, have the disadvantage that an increasing amount of the heat flow curve is truncated, while the minimum width of calculation window is the maximum value of the switching time range in order to ensure that at least one whole temperature pulse is included in any evaluation. For this reason, heat flow evaluations in TOPEM are performed width of calculation window is the a maximum of 120 s, which necessarily restricts the TOPEM experiment to a switching time range with a maximum value less than 120 s, while the frequency evaluations can be made for greater window widths.

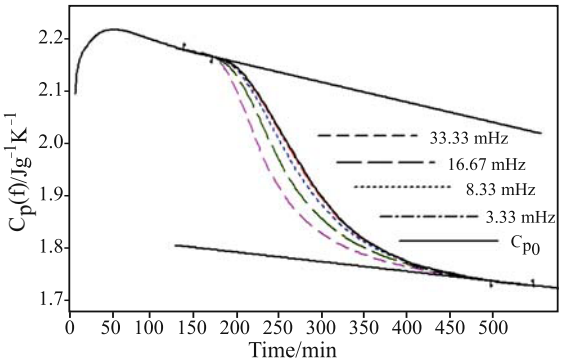

Fig. 4 Frequency dependent $C_p(f)$ curves as a function of time obtained by the frequency evaluation of the C_{p0} curve. Note that the frequency curve for 3.33 mHz superposes almost exactly upon the curve for C_{p0}, and hence is barely visible

Table 2 Dynamic vitrification time (in minutes) as a function of frequency (or period, in s, shown in parentheses) for quasi-isothermal TOPEM experiments at 50 and 70°C, for the switching times indicated. Two separate experiments [(a) and (b)] with the same switching time range 15–30 s were performed at 70°C

f/mHz	50°C	70°C			
	15–30 s	15–30 s (a)	15–30 s (b)	15–300 s	15–900 s
120	362.2	–	–	201.3	202.9
100 (10)	367.6	–	–	204.5	205.6
66.7 (16)	382.5	–	–	210.9	210.3
50 (20)	389.7	224.3	225.8	214.1	213.8
33.3 (30)	396.6	236.7	231.0	216.6	222.8
16.7 (60)	414.5	258.0	248.9	232.8	243.0
8.3 (120)	430.7	274.7	262.9	245.5	252.5
3.3 (300)	437.2	283.1	268.3	249.8	256.0
1.7 (600)	438.0	284.0	269.1	250.5	256.6
1.1 (900)	438.1	284.2	269.2	250.6	256.7

Table 3 Partial heats of cure, residual heats of cure and total heats of cure and glass transition temperatures of fully cured samples for the ADSC and TOPEM isothermal cure experiments at 50 and 70°C

Experiment	Heats of cure/J g^{-1}			T_g/°C
	partial	residual	total	
ADSC 50°C	363.2	50.5	413.7	87.6
ADSC 70°C	418.8	11.4	430.2	87.5
TOPEM 50°C	364.0	59.4	423.5	87.8
TOPEM 70°C (a)	386.5	7.0	393.5	81.6
TOPEM 70°C (b)	395.8	6.5	402.2	84.8

Data analysis

The partial heats of curing during the quasi-isothermal ADSC and TOPEM experiments and their corresponding residual and total heats of cure from the second scans are summarized in Table 3. For the reasons given above, these values were obtained from ADSC experiments with a period of 60 s and from TOPEM experiments with a switching time range of 15–30 s and a calculation window width of 120 s. The rate of cure is calculated from the equation:

$$\frac{d\alpha}{dt}=\frac{\phi}{\Delta H_{tot}} \quad (1)$$

where ϕ is the heat flow at time t and ΔH_{tot} is the total heat of cure, being the sum of the partial and residual heats of cure. The degree of cure, α, at any time t is then found simply as the area under the heat flow curve up to that time, normalised by the total heat of cure. A typical representation of the rate of cure as a function of the degree of cure is shown for a TOPEM experiment at 50°C the open circles in Fig. 5.

The kinetic analysis of the major part of the cure process which is controlled by chemical reaction is based upon the equation of Kamal [14]:

$$\frac{d\alpha}{dt}=(k_1+k_2\alpha^m)(1-\alpha)^n \quad (2)$$

where k_1 and k_2 are rate constants with an Arrhenius temperature (T) dependence and the exponents m and n are the reaction orders. This kinetic model has been used to fit the experimental data within the range in which the reaction is chemically controlled. An illustration of this fit is shown as the full line in Fig. 5. It is clear that a good fit is obtained for the majority of the reaction, but that a significant deviation occurs in the region of α=0.8, where the experimental data decrease rather rapidly to zero at a value of α less than unity, while the theoretical curve continues to reach zero at α=1. This deviation represents the effect of vitrification.

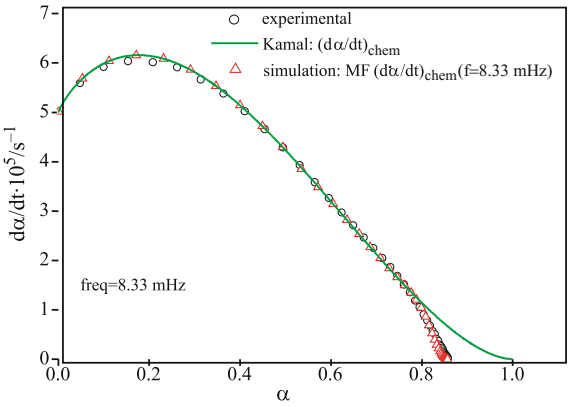

Fig. 5 Rate of cure as a function of α obtained experimentally at 50°C (open circles), showing vitrification in the range of $\alpha\approx$0.8. The full line is the fit of the theoretical model, Eq. (2), to the chemically controlled region up to vitrification. The open triangles represent the fit to the whole of the reaction using Eq. (3) with DF=MF for f=8.33mHz

In view of the fact that the rapid decrease in the rate of cure that occurs when vitrification intervenes is as a result of a change in the kinetics from a chemically controlled rate to one that is diffusion controlled, it is common to quantify the effect of vitrification by means of the diffusion factor (DF) [15]:

$$\left(\frac{d\alpha}{dt}\right)_{exp}=DF\left(\frac{d\alpha}{dt}\right)_{chem} \quad (3)$$

which relates the experimentally measured reaction rate, $(d\alpha/dt)_{exp}$, to the theoretical chemical reaction rate, $(d\alpha/dt)_{chem}$, according to the appropriate model (Eq. (2) in the present case). Thus the diffusion factor must take a value of unity in the region in which the reaction is controlled chemically, and then falls to zero when vitrification occurs. One way that has been proposed [5, 6] for modelling this effect of vitrification is by means of a mobility factor (MF) which can be determined directly from the experimental data, for any cure temperature, from the time dependence of the complex heat capacity curve for any frequency, f, such as that shown in Fig. 1. The mobility factor can be described by the following equation:

$$MF(f)=\frac{[C_p^*(t,f)-C_{pg}^*(t,f)]}{[C_{pl}^*(t,f)-C_{pg}^*(t,f)]} \quad (4)$$

where C_{pl} and C_{pg} are the (time- and frequency-dependent) heat capacities of the asymptotic liquid and glassy regions, respectively, for a given cure temperature, T_c, as shown in Fig. 1. The mobility factor therefore, like the diffusion factor, must decrease from unity to zero as the vitrification process occurs, and for this reason has been suggested to be an approximation to the DF. Unlike the DF, however, the MF is dependent on the frequency, since t_v is frequency-dependent (Tables 1

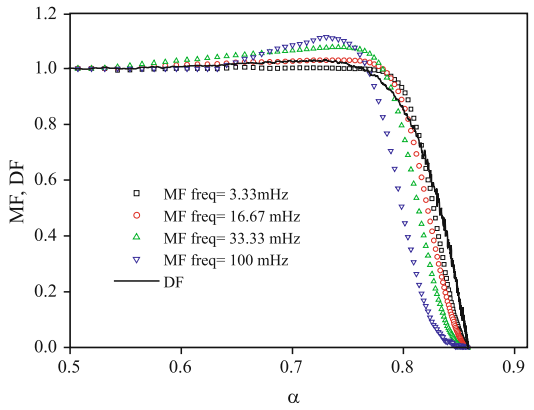

Fig. 6 Dependence of MF, from the TOPEM quasi-isothermal cure experiment at 50°C, on time of cure for selected frequencies, and the comparison with the DF

and 2). It is interesting, therefore, to examine the extent to which the two factors, DF and MF, are indeed comparable in any given isothermal curing experiment. To do so, the MF is calculated from the complex heat capacity C_p^* data of ADSC or from the frequency-dependent $C_p(f)$ data of TOPEM according to Eq. (4), and compared with the DF calculated from Eq. (3) and the fit of the Kamal equation (Eq. (2)) to the chemically controlled part of the cure.

This approach has been applied to the TOPEM data for frequencies from 1.1 to 120 mHz. The dependence of MF on degree of cure for selected frequencies within this range at a cure temperature of 50°C is shown in Fig. 6, and compared with the DF for this same isothermal cure experiment. Alternatively, assuming that the MF is a good approximation to the DF, one can apply these experimentally calculated mobility factors in the place of the diffusion factor in Eq. (3) in order to model the effect of vitrification on the cure curves of dα/dt *vs.* α for each frequency. The results are shown as open triangles in Fig. 5 for one selected frequency (8.33 mHz). Although the fit of the whole cure reaction making use of Eq. (3) appears rather good, the region of particular interest is that in which vitrification occurs. In order to examine the vitrification in more detail, an enlarged view of this region is presented in Fig. 7 for five frequencies: 8.3, 16.7, 33.3, 50 and 100 mHz.

Discussion

The use of the mobility factor to model cure in which vitrification takes place has not always been successful. Although there appears to be a good approximation between the diffusion factor and MF for a period of 60 s for epoxy–amine reactions [5–7], it has been shown to be inadequate for others, such as epoxy–anhydride systems [8]. Furthermore, there is

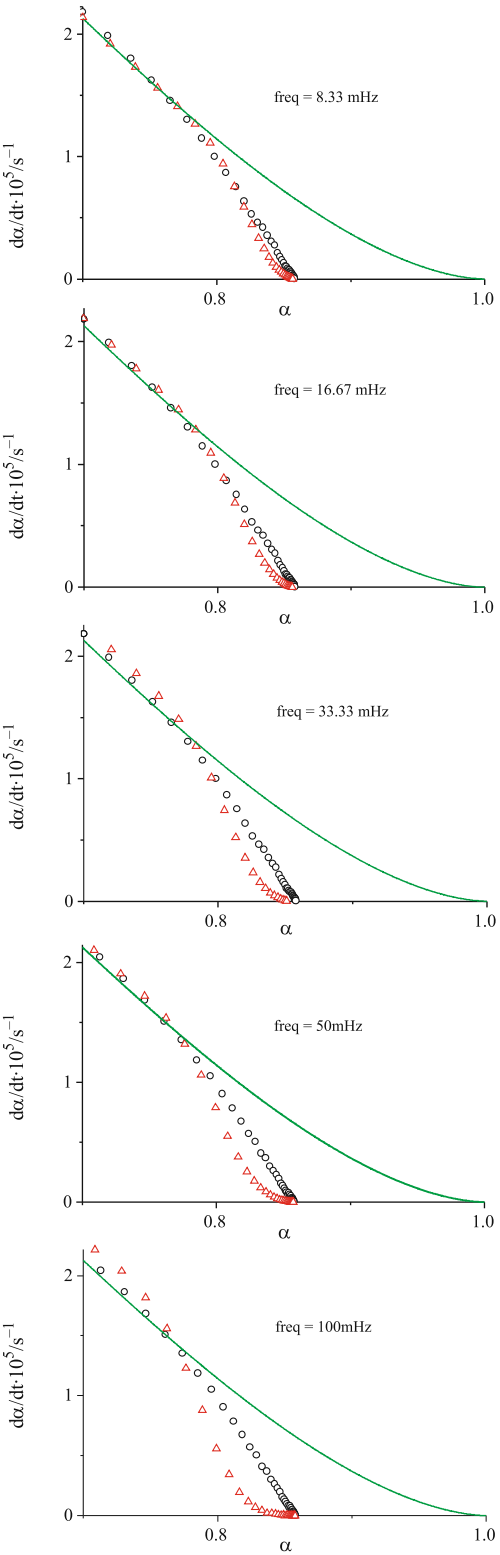

Fig. 7 Enlarged views of the vitrification region in isothermal cure at 50°C by TOPEM. The open circles represent the experimental data. The full line is the fit of the Kamal model (Eq. (2)) to the chemically controlled region up to the start of vitrification. The open triangles are obtained by using Eq. (3) in which DF=MF, with MF corresponding to the frequencies indicated

also the question of the role of the frequency of modulation. The suggestion has been made that its applicability for a period of 60 s in epoxy–amine systems is fortuitous, and that at other frequencies, and in particular at higher frequencies, significant deviations would be observed.

The use of TOPEM, in which only a single sample is required in order to obtain frequency-dependent data for the confirmation or otherwise of this suggestion, represents a useful advantage over ADSC. Examining the results shown in Fig. 7 for the region in which vitrification occurs, it can indeed be seen that the quality of fit of the theoretical model applied to the whole of the reaction by means of the DF as in Eq. (3), and using MF defined by Eq. (4) as an approximation to DF, depends on the frequency. The differences between DF and MF are even more marked when these two factors are viewed together as a function of the degree of cure, as in Fig. 6.

This is, in fact, what one might expect. The dependence of the rate of cure on the degree of cure, as represented in Fig. 5, is found from the total heat flow data, which are frequency-independent. On the other hand, the mobility factor is frequency-dependent, as shown in Fig. 6, and as a consequence gives rise to the deviations seen in Fig. 7. Nevertheless, there is in fact rather a good agreement between DF and MF in the range of the lowest frequencies used here, corresponding to modulation periods of about 60 s (f=16.7 mHz), the difference between DF and MF becoming greater as the frequency increases. Why this should be so is an interesting question, particularly in view of the fact that in epoxy–anhydride systems shorter modulation periods than 60 s are necessary in order to achieve a satisfactory correspondence between DF and MF [8]. Likewise, if the curing reaction is studied by dielectric analysis rather than by TMDSC techniques, in other words at much higher frequencies, and if vitrification is associated with the step change in the permittivity (or the peak in the loss factor) instead of the step change in the complex heat capacity, then the vitrification time would be much shorter and the degree of cure at vitrification would be significantly smaller. This would imply that the vitrification process identified by dielectric analysis at high frequencies is very different from that occurring in the regime in which the chemically controlled reaction is changing to one controlled by diffusion, as has been pointed out before [16]. Under these circumstances, what is being observed by dielectric analysis is the frequency-dependent ('dynamic') glass transition or α-relaxation of the partially cured system. In fact, this is also what is observed by TMDSC techniques, but since the frequency is much lower, the dynamic vitrification time identified by the step change in C_p^* is much longer, as can be seen by comparing the dynamic vitrification times from dielectric analysis and TMDSC in [17], though these authors do not make this comparison. Hence, in TMDSC the cure will have proceeded further by this time, and often to such an extent that the degree of cure corresponds approximately to that at which the frequency-independent change from a chemically controlled to a diffusion controlled reaction occurs. It would appear, therefore, that in the epoxy-amine system studied in the present work the relatively good agreement between DF and MF occurs just in the range of frequencies in which TMDSC techniques are usually applied.

This approximate correspondence between a frequency-dependent (from C_p^* by TMDSC) and a frequency-independent (from the DSC heat flow) vitrification time is similar to the well-established relationship between the dynamic and thermal glass transitions in amorphous polymers [9, 10]. The dynamic glass transition, as observed by TMDSC techniques, is dependent on the frequency of modulation. On the other hand, the thermal transition, as observed typically in conventional DSC, is dependent on the cooling rate. It transpires that, at least for many polymers, these two transition temperatures are not very far apart for the usual ranges of cooling rates and frequencies applied in DSC and TMDSC, respectively. Indeed, this is to a certain extent a problem when it is desired to study the dynamic glass transition without any interference from the thermal transition. Furthermore, it is possible to relate the cooling rate and frequency required in order to obtain the same glass transition temperature by DSC and TMDSC, a relationship that can be interpreted in terms of fluctuation dissipation theories [18, 19] and which is significantly different for different glass-forming systems. It would seem that an analogous effect is being observed in the present studies of vitrification during isothermal cure. For epoxy-amine systems, the dynamic vitrification process appears to coincide reasonably well with the thermal vitrification for modulation periods typical of TMDSC techniques, for example 60 s. On the other hand, for the epoxy–anhydride system a different frequency range is appropriate [8].

The frequency dependence of the dynamic vitrification time is in itself interesting. A plot of t_v *vs.* the frequency on a logarithmic scale for the results obtained by ADSC (Table 1) and TOPEM (Table 2) is shown in Fig. 8. The first point to note is that the TOPEM data level off for frequencies less than approximately 5 mHz. An analogous observation was previously made in the study of the frequency dependence of the dynamic glass transition in polycarbonate [13], where TOPEM data yielded

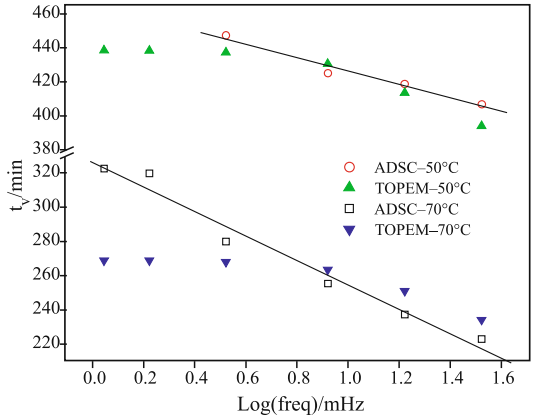

Fig. 8 Vitrification time, t_v, *vs*. log(frequency) for ADSC (open symbols) and TOPEM data (filled symbols) at 50°C (upper set of data) and 70°C (lower set of data). The straight lines are least squares fits to the ADSC data

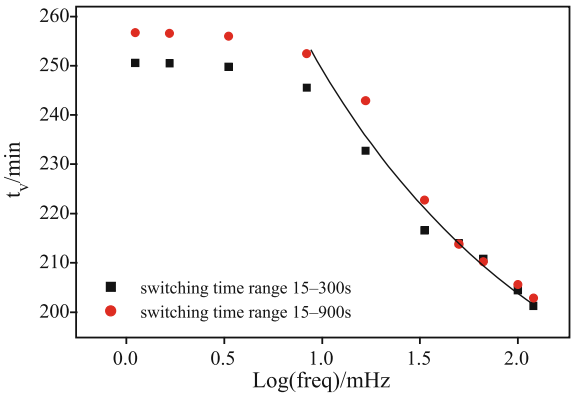

Fig. 9 Vitrification time, t_v, *vs*. log(frequency) for TOPEM experiments at 70°C. The curve is drawn to guide the eye

dynamic glass transition values which were independent of frequency for frequencies below about 4 mHz, and this represents a current limitation in the range of frequencies able to be evaluated by TOPEM. Leaving aside this limitation of the TOPEM data, though, it can be seen that the data for TOPEM and ADSC superpose within the errors associated with such measurements. It is particularly noticeable that the scatter of the TOPEM data is less than that for the ADSC data, which can be attributed to the elimination, in the former, of an important possible source of experimental error, namely the variation in the sample due to the preparation of a fresh resin/diamine mixture for each ADSC experiment with different modulation periods. A linear least squares fit to each set of ADSC data at the two cure temperatures of 50 and 70°C is shown in Fig. 8, from which it can be seen that the dependence of t_v on log$f$ is stronger the higher is the cure temperature, as is commonly observed [16].

The highest frequency shown in Fig. 8 corresponds to a period of 30 s, which is the shortest period that can be achieved in practice with ADSC while the sample follows the temperature modulations. With TOPEM, it is possible to achieve higher frequencies as a result of the data analysis procedure, which is based upon a transfer function between the imposed stochastic temperature pulses and the corresponding measured heat flow response. This extension of TOPEM data to higher frequencies combined with the reduction in scatter in comparison with the ADSC data allows us to infer that the relationship between t_v and log$f$ at the higher end of the frequency range, as shown in Fig. 9, appears to have some upward curvature, as indicated by the smooth curve that is drawn through the points to guide the eye. These data correspond to those reported in Table 2 for switching time ranges of 15 to 300 and 15 to 900 s. It was not possible to obtain satisfactory results at frequencies higher than 50 mHz for TOPEM experiments with a switching time range of 15 to 30 s, as represented by the lack of data for these frequencies in Table 2. It appears that, for TOPEM, higher frequencies can be evaluated when the switching time range is broader.

The observation of some upward curvature in the data presented in Fig. 9 is different from the situation reported at much higher frequencies and obtained by dielectric analysis (DEA) [16, 20, 21], in which region a linear equation relating t_v and log$f$ has been proposed [20], which may be written as follows:

$$t_v = -t_0 \log(f/f_0) \qquad (5)$$

where t_0 and f_0 are constants. Interestingly, though, in experiments in which both DEA and ADSC (with a period of 60 s) were used to study the vitrification of an epoxy-amine system [21], the linear extrapolation of the high frequency DEA data to the frequency range of ADSC did not pass through the single data point at 60 s for any cure temperature except the lowest. This suggests that in general there is an upward curvature to these plots, such as is seen in Fig. 9, in the range of frequencies where ADSC and TOPEM are employed. In the second part of this paper, we present a theoretical model for the vitrification process and a prediction of the frequency dependence of the dynamic vitrification time, as determined by temperature modulated DSC techniques, in which these observations are explained.

Conclusions

The use of TOPEM in studying the vitrification process during the isothermal cure of thermosetting resins presents a significant advantage over other temperature modulated DSC techniques, such as ADSC, in that a single experiment permits the evaluation of the dynamic vitrification time for a range of frequencies. Not only is this convenient in respect of its significant

time savings, but also it reduces the experimental errors involved in that only a single sample is used. Nevertheless, there still remains a limitation to the TOPEM technique in that the minimum frequency currently available is about 5 mHz.

It is shown, by TOPEM that the use of the mobility factor leads only to an approximation to the experimental cure rate during vitrification. This is attributed to the fact that the mobility factor is frequency-dependent, as a result of the frequency dependence of the dynamic vitrification time, so that the predicted cure rate curve during vitrification also depends on the frequency, unlike the experimental curve which is frequency-independent.

The dependence of dynamic vitrification time on log(frequency) appears to show a slightly non-linear behaviour, with an upward curvature. This is consistent with an earlier result which compared dynamic vitrification times measured in distinctly different frequency ranges, relatively low frequencies for TMDSC techniques on the one hand and relatively high frequencies for dielectric analysis on the other. The reason for this is explored in the second part of this series.

Acknowledgements

The authors are grateful for the provision of equipment and technical advice from Mettler-Toledo. JMH is grateful for a Ramón y Cajal research grant. Financial support has been provided by CICYT, Project MAT 2004-04165-C02-01. We are grateful to Huntsman for the provision of the Jeffamine D-230 curing agent.

References

1 A. T. DiBenedetto, in L.E. Nielsen Ed., J. Macromol. Sci. Rev. Macromol. Chem., C3 (1969) 69.
2 J. K. Gillham, Polym. Eng. Sci., 26 (1986) 1429.
3 S. Montserrat, J. Thermal Anal. 37 (1991) 1751.
4 M. Cassettari, G. Salvetti, E. Tombari, S. Veronesi and G. P. Johari, J. Polym. Sci: Polym Phys., 31 (1993) 199.
5 G. Van Assche, A. Van Hemelrijck, H. Raier and B. Van Mele, Thermochim. Acta, 268 (1995) 121.
6 A. Van Hemelrijck and B. Van Mele, J. Thermal Anal., 49 (1997) 437.
7 S. Montserrat and I. Cima, Thermochim. Acta, 330 (1999) 189.
8 S. Montserrat and X. Pla, Polym. Int., 53 (2004) 326.
9 S. Montserrat, Y. Calventus and J. M. Hutchinson, Polymer, 46 (2005) 12181.
10 S. Weyer, H. Huth and C. Schick, Polymer, 46 (2005) 12240.
11 F. Román, S. Montserrat and J. M. Hutchinson, J. Therm. Anal. Cal., 87 (2007) 113.
12 J. E. K. Schawe, T. Hütter, C. Heitz, I. Alig and D. Lellinger, Thermochim. Acta, 446 (2006) 147.
13 I. Fraga, S. Montserrat and J. M. Hutchinson, J. Therm. Anal. Cal., 87 (2007) 119.
14 M. R. Kamal, Polym. Eng. Sci., 14 (1974) 231.
15 K. C. Cole, J. J. Hechler and D. Noël, Macromolecules, 24 (1991) 3098.
16 J. Fournier, G. Williams, C. Duch and G. A. Aldridge, Macromolecules, 29 (1996) 7097.
17 L. Núñez-Regueira, S. Gómez-Barreiro and C. A. Gracia-Fernández, J. Therm. Anal. Cal., 82 (2005) 797.
18 A. Hensel, J. Dobbertin, J. E. K. Schawe, A. Boller and C. Schick, J. Thermal Anal., 46 (1996) 935.
19 E. Donth, The glass transition. Relaxation Dynamics in Liquids and Disordered Materials. Springer, Berlin 2001.
20 M. B. M. Mangion and G. P. Johari, J. Polym. Sci. Polym. Phys., 28 (1990) 1621.
21 S. Montserrat, F. Román and P. Colomer, Polymer, 44 (2003) 101.

Received: July 3, 2007
Accepted: July 17, 2007

DOI: 10.1007/s10973-007-8613-7